Journal of Hazardous Materials 186 (2011) 206–211

Contents lists available at ScienceDirect

Journal of Hazardous Materials

journal homepage: www.elsevier.com/locate/jhazmat

Sorption of nitrate onto amine-crosslinked wheat straw: Characteristics, column sorption and desorption properties

Xu Xing, Bao-Yu Gao*, Qian-Qian Zhong, Qin-Yan Yue, Qian Li

Key laboratory of water pollution control and recycling (Shandong), School of Environmental Science and Engineering, Shandong University, Jinan 250100, PR China

ARTICLE INFO

Article history:
Received 6 September 2010
Received in revised form 26 October 2010
Accepted 27 October 2010
Available online 2 November 2010

Keywords:
Nitrate
Column
Desorption
Raman spectrum
Wheat straw

ABSTRACT

The nitrate removal process was evaluated using a fixed-bed column packed with amine-crosslinked wheat straw (AC-WS). Column sorption and desorption characteristics of nitrate were studied extensively. Solid-state ^{13}C NMR and zeta potential analysis validated the existence of crosslinked amine groups in AC-WS. Raman shift of the nitrate peaks suggested the electrostatic attraction between the adsorbed ions and positively charged amine sites. The column sorption capacity (q_{ed}) of the AC-WS for nitrate was 87.27 mg g^{-1} in comparison with the raw WS of 0.57 mg g^{-1}. Nitrate sorption in column was affected by bed height, influent nitrate concentration, flow rate and pH, and of all these, influent pH demonstrated an essential effect on the performance of the column. In addition, desorption and dynamic elution tests were repeated for several cycles, with high desorption rate and slight losses in its initial column sorption capacity.

1. Introduction

The wastes of the production in pharmaceuticals, fertilizer, food service, and explosive industries are nitrate bearing wastes [1]. Oxides of nitrogen, such as nitrate and nitrite are common pollutants in closed surface water systems and ground water. The release of nitrogenous compounds from wastewaters to the environment is undesirable because it provides an excess of nutrients in the natural water bodies and accelerates eutrophication. What's more, high concentrations of N-containing compounds in drinking water cause health problems such as cyanosis among children and cancer of the alimentary canal [2,3]. Therefore, removal of nitrate and nitrite from water is of significant important from the environmental and health point of view.

Despite the environmental and health benefits of limiting nitrate and nitrite release, there is a continuous need to supply nitrogen to agriculture and industry. Thus, development of treatment methods that facilitate the removal of nitrate from wastewaters prior to discharge into natural waters is required.

In wastewater treatment technology, various techniques for the removal of nitrate and nitrite from water have been reported in a number of publications. These include biological denitrification [4,5], chemical reduction [6], electrodialysis [7], bioelectrochemical [8] and adsorption [9,10]. Of all these, adsorption is well recognized as one of the simplest and safest methods used for the removal of nitrate from wastewater. Recently, numerous attempts have been made in finding inexpensive and effective adsorbents produced from agricultural by-products. Studies showed that many materials, such as sugarcane bagasse, peanut hull, sawdust, coconut husk and pine bark could be modified into anion exchangers and utilized for this purpose [11–15]. The agricultural by-product represents a potential alternative as an adsorbent because of its particular properties such as its chemical stability and high reactivity, resulting from the presence of reactive hydroxyl groups in cellulose/hemicellulose chains [16,17].

In our previous work for preparation of the adsorbent, the aminated intermediate method was presented, which comprised first preparation of the aminated intermediate by reaction of epichlorohydrin with triethylamine, and then introduction of the aminated intermediate into the agricultural by-products in the presence of a catalyst [18]. In this work, a new kind of adsorbent was prepared from wheat straw (WS) by WS crosslinked first. The amine-crosslinked wheat straw (AC-WS) was measured by zeta potential, solid-state ^{13}C NMR and Raman spectrum techniques and the physicochemical and sorption properties of the adsorbent were characterized. Sorption characteristics of AC-WS in fixed-bed column were studied by varying the influent conditions in the continuous system such as bed height, influent nitrate concentrations, flow rates and influent pH. What's more, desorption and dynamic elution tests were repeated in four sorption–desorption cycles to evaluate the regeneration property of AC-WS using HCl as the desorption agent.

* Corresponding author. Tel.: +86 531 88364832; fax: +86 531 88364513.
E-mail address: bygao@sdu.edu.cn (B.-Y. Gao).

0304-3894/$ – see front matter © 2010 Elsevier B.V. All rights reserved.
doi:10.1016/j.jhazmat.2010.10.104

2. Materials and methods

2.1. Materials

WS was obtained from Liao Cheng, Shandong, China. The raw WS was pretreated in the biomass pool for three months so that the intertwined cellulose, hemicellulose and lignin chains in WS could be degraded. The fermented WS was washed with water, dried at 60 °C for 6 h and sieved into particles with diameters from 100 to 250 μm.

2.2. Preparation of AC-WS

Ten gram of WS was reacted with 10 ml of epichlorohydrin and 9 ml of N, N-dimethylformamide in a three-neck round bottom flask at 85 °C for 60 min. Three millilitres of ethylenediamine was added and the mixture was stirred for 45 min at 85 °C, followed by adding 9 ml of triethylamine for grafting and stirring for 120 min at 85 °C. The product was washed with 250 ml of distilled water to remove the residual chemicals, dried at 60 °C for 12 h and sieved to obtain particles smaller than 250 μm in diameter.

The synthetic reactions for the anion exchange resins utilizing WS as a starting material are depicted in Fig. 1. As is shown in Fig. 1, the synthetic reactions are the chain reactions between the cellulose/hemicellulose chains and side chains of different grafting chemical reagents. The synthetic reactions have been separated into three steps. In the first step, epichlorohydrin is attached to the cellulose/hemicellulose chains and forms the side chains after the reaction with hydroxyl, producing the epoxy cellulose/hemicellulose ethers [12,13]. The epoxy ethers are hydrolyzed and then the chains are cross-linked with ethylenediamine to produce diamine cellulose/hemicellulose ethers [18,19]. In the third step, the triethylamine is grafted onto the diamine cellulose/hemicellulose ethers and form the triethyl ammonium sites in an excess of epichlorohydrin [20].

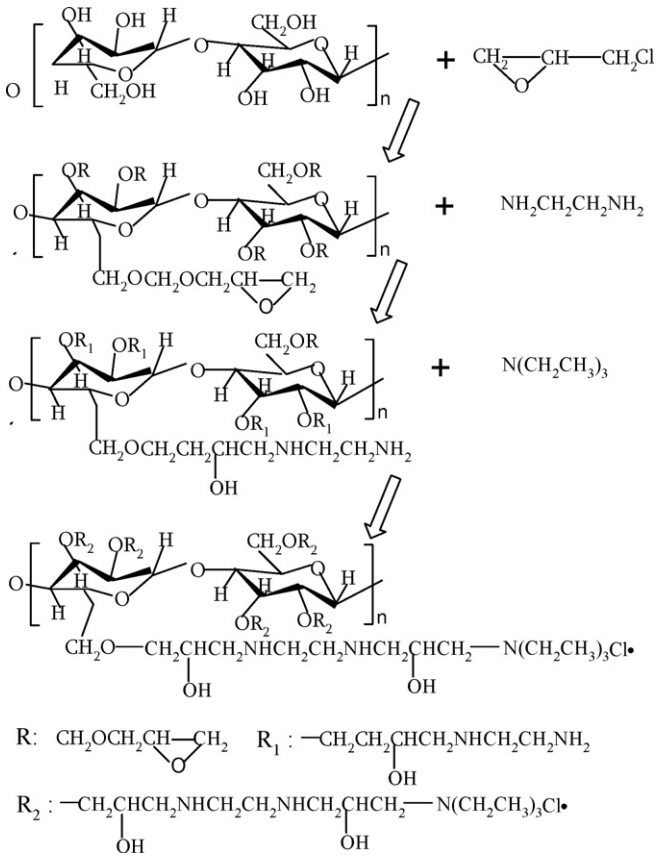

Fig. 1. Chain reaction between cellulose/hemicellulose chains and grafting chemical reagents.

2.3. Solid-state ^{13}C NMR, zeta potential and Raman spectroscopic analysis

Solid-state ^{13}C NMR spectra have been used in our previous work [21]. Solid-state ^{13}C NMR spectra were acquired at room temperature on a Varian 400 Unity Inova spectrometer operating at 100.57 MHz and equipped with a 4 mm probe-head. All ^{13}C spectra were recorded under magic angle spinning (MAS) conditions at a spinning speed of 14 kHz. Improvements in the signal-to-noise ratio were gained using cross-polarisation (CP) to transfer magnetization from proton to carbon. CP experiments were performed using a 2 s recycle delay and a 1000 μs contact time.

Zeta potential measurements were carried out using a micro-electrophoresis apparatus (JS94H, Shanghai Zhongchen Digital Technical Apparatus Co., Ltd, China). The AC-WS or WS samples were prepared in 25 ml of distilled water containing 0.1 g of AC-WS or WS. In addition, the nitrate-loaded AC-WS samples were prepared by maintaining the suspension contained with 0.1 g of AC-WS and 100 mg l^{-1} nitrate. The initial pH of the suspensions was adjusted between 2 and 12 and they were mixed for 24 h. Then, the zeta potential of the samples and final pH of the suspension was measured.

Raman spectroscopic analysis was performed to provide insights into the mechanisms of nitrate interactions with AC-WS. In the Raman analysis, 0.1 g AC-WS was placed in 50 ml of nitrate solution with concentration of 0.5 mol l^{-1}. The wet solid samples and nitrate of potash solution (0.5 mol l^{-1}) were analyzed by Raman spectroscopy (Nicolet Almega XR Dispersive Raman, Thermo Electron Corporation, USA). The laser wavelength used in Raman measurement was 1050 nm.

2.4. Column sorption tests

A fixed-bed column with 200 mm length and 12 mm diameter was used in the column sorption/desorption tests. Sorption characteristics of AC-WS in fixed-bed column were studied by varying the bed height (1.0, 1.5 and 2.5 cm), influent nitrate concentrations (80, 120, 200 and 300 mg l^{-1}), flow rates (3.3, 5, 10 and 15 ml min^{-1}) and influent pH (2.21, 4.97, 7.15, 10.16 and 11.89), respectively. The effluent solutions were collected, and every 10 ml was selected as a sample to determine the residual concentrations in the effluent solutions. The flow to the column was continued until the effluent nitrate concentration (C_t) approached the influent concentration (C_0), $C_t/C_0 = 0.98$. Nitrate solutions were prepared by high purity water, and its normal pH value is about 5.12. The nitrate concentration was determined spectrophotometrically according to the Brucine-sulfanil colorimetric method, using a UV–visible spectrophotometer (model UV754GD, Shanghai).

The column sorption capacity (q_{ed}) was calculated by the equation expressed as:

$$q_{ed} = \frac{c_o V_o - \sum c_n v_n}{m} \quad (1)$$

where q_{ed} is the amount of nitrate sorption per gram AC-WS at saturation (mg g^{-1}), c_o is the original concentration (mg l^{-1}), V_o is the total volume of the influent solutions (L), c_n is the concentration of sample n (mg l^{-1}), and v_n is the volume of sample n (L), m is the amount of AC-WS (g).

2.5. Desorption tests in column

Regeneration of the AC-WS as well as recovery of adsorbate material was achieved by eluting the hydrochloric acid (HCl) solution through the exhausted column. The sorption–desorption cycles were carried out for four times. The eluted nitrate concentrations and the q_{ed} in each cycle were calculated.

3. Results and discussion

3.1. Characteristics of AC-WS

3.1.1. Solid-state ^{13}C NMR spectra of WS and AC-WS

Fig. 2 shows the solid-state ^{13}C NMR spectra of WS and AC-WS. The spectra of cellulose/hemicellulose chains in WS are dominated by the set of resonances in the region between 60 and 120 ppm [22]. As seen in Fig. 2a, a set of five distinct peaks were present. The intense peak at 105, 84 and 64 ppm is assigned to C-1, C-5 and C-6 carbons in cellulose chains and 103, 82 and 62 ppm correspond to C-1, C-5 and C-6 carbons of hemicelluloses (cellulose and hemicelluloses use the same monomer in Fig. 2a). The intense peaks at 73 and 75 ppm are overlapping signals due to the C-2, C-3, and C-5 carbons of all polysaccharides [23–25].

Solid-state ^{13}C NMR spectra of AC-WS are shown in Fig. 2b. Enlargement of amine carbon peaks (30–60 ppm) are observed in spectra of AC-WS as compared to the spectra of WS, which is the result of the presence of the carbons of $-CH_2N-$ and $-NCH_3$. The central chemical shifts for the peaks of $-CH_2N-$ and $-NCH_3$ are located at 52 ppm and 35 ppm, respectively. Nevertheless, these signals are accounted together with the carbons of celluloses and hemicelluloses, which make it difficult to quantify each component [24].

3.1.2. Zeta potential analysis

Zeta potentials of WS, AC-WS and nitrate-loaded AC-WS as a function of pH are shown in Fig. 3. The zeta potentials of WS samples decrease from 2.2 mV to −46.3 mV as the initial pH of the suspensions increases from 2.0 to 12.0. In contrast with the WS samples, the zeta potentials of AC-WS are in the range of −7.0 to +35.3 mV in designed pH range; this indicates the existence of positive-charge functional groups on the framework of AC-WS. The decrease in zeta potentials of these samples as a function of pH could be attributed to the pH-dependent functional groups existing in WS and AC-WS, such as hydroxyl and carboxyl groups. These groups will exhibit a greater negative charge as the pH increases and result in the decrease of the positive charge in WS and AC-WS.

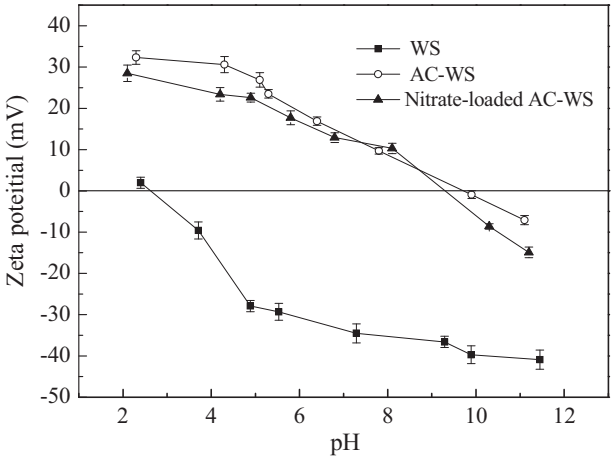

Fig. 3. Zeta potentials of WS, AC-WS and nitrate-loaded AC-WS as a function of pH.

A slight decrease in zeta potentials of nitrate-loaded AC-WS is observed as compared to those of AC-WS. The removal of nitrate involves exchange of nitrate with chloride on the AC-WS. The decreased zeta potential in nitrate-loaded AC-WS could be attributed to displacement of chloride anion by an adsorbed nitrate anion due to steric effects [26]. Similar result was reported in the work of Yoon for the sorption of perchlorate by resin and active carbon [26].

3.1.3. Raman spectrum

Fig. 4a–c, present the Raman spectrums of nitrate solution, AC-WS and nitrate-loaded AC-WS, respectively. Appearance of peaks at 2800–3000, 1590–1620 and 1450–1470 cm^{-1} are the characteristic peaks of cellulose/hemicellulose chains in AC-WS [27]. A new peak at 1043.3 cm^{-1} is observed in the spectrum of nitrate-loaded

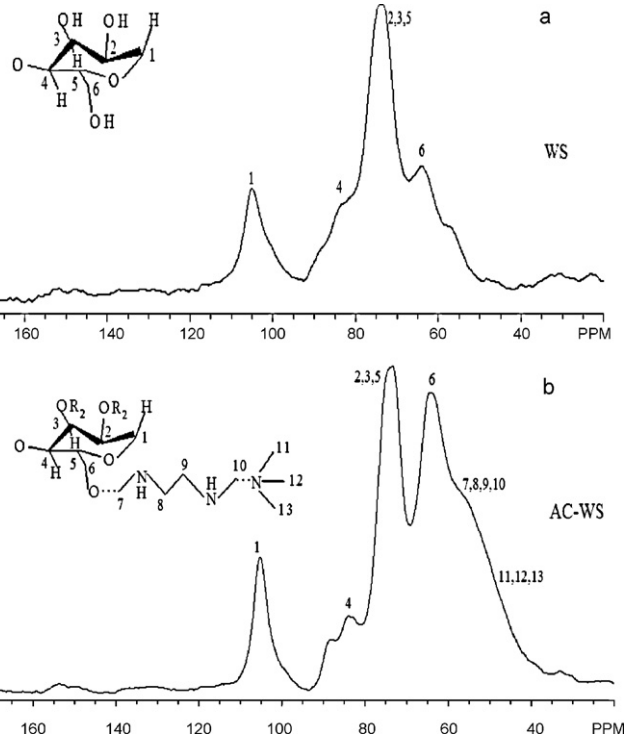

Fig. 2. Solid-state ^{13}C NMR spectra of WS and AC-WS.

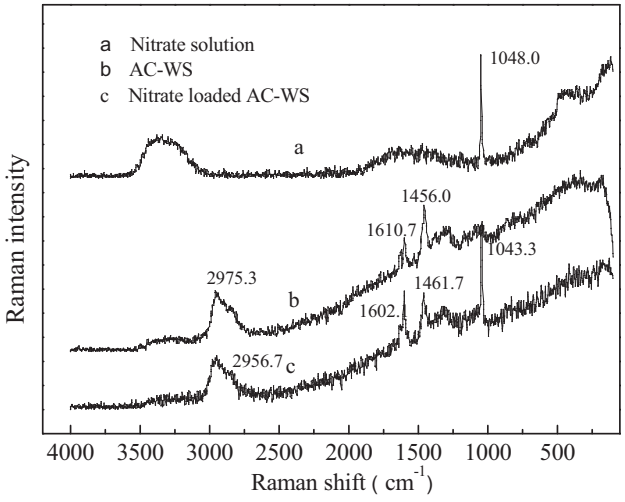

Fig. 4. Raman spectrums of nitrate solution, AC-WS and nitrate-loaded AC-WS.

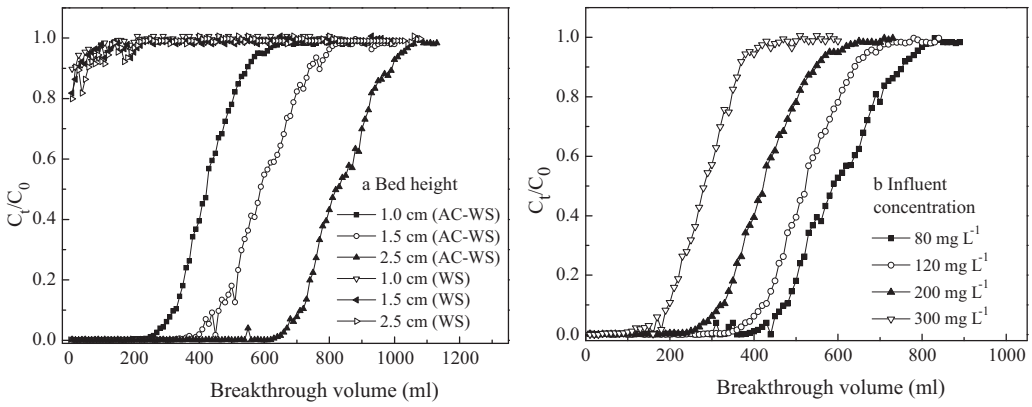

Fig. 5. Effect of bed height and influent concentration on the breakthrough curves. (a) Influent concentration: 200 mg l^{-1}, influent pH: 5.12, flow rate: 5 ml min^{-1}; (b) bed height: 1.0 cm, influent pH: 5.12, flow rate: 5 ml min^{-1}.

AC-WS as compared to that of AC-WS, attributed to the adsorbed nitrate on the surface of AC-WS.

Nitrate in a 0.5 mol l^{-1} of nitrate of potash solution has a characteristic peak at 1048 cm^{-1} (Fig. 4a). Oliveira reported a peak at 1049 cm^{-1} for an aqueous nitrate solution (0.5 mol l^{-1} of $NaNO_3$) [28]. It is observed that the peak in the spectrum of adsorbed nitrate agrees with the characteristic peak of the free nitrate ion in solution, indicating that there is no strong chemical interaction between the adsorbed nitrate and the AC-WS [26,29]. It suggests that nitrate is adsorbed onto the AC-WS surface through electrostatic attraction between the nitrate ions and the positively charged amine sites. Therefore, the peak assignments of nitrate solution and adsorbed nitrate in AC-WS are both free anions and the mechanism of nitrate species sorption by the AC-WS may be proposed as in Eq. (2).

$$R\text{–}N^{+}(CH_2CH_3)_3 \ldots Cl^{-} + NO_3{}^{-} \rightarrow R\text{–}N^{+}(CH_2CH_3)_3 \ldots NO_3{}^{-} + Cl^{-} \quad (2)$$

3.2. Column sorption tests

When the sorption zone moves up and the upper edge of this zo ne reaches the bottom of the column, the effluent concentration starts to rise rapidly. This is called the breakthrough point. The desired breakthrough point is determined to be 0.1 C_t/C_0. The point where the effluent nitrate concentration reached 95% ($C_t/C_0 = 0.95$) of its influent value is called the point of column exhaustion [30].

3.2.1. Effect of bed height on the column sorption of AC-WS and WS

The results in Fig. 5a present the column sorption of AC-WS and WS at different bed heights. The mass for 1.0, 1.5 and 2.5 cm of bed heights are about 1.0 g, 1.5 g and 2.5 g of AC-WS and 0.8, 1.2 and 2.0 g of WS, respectively. The influent solution was infused into the fixed bed column with nitrate concentration of 200 mg P l^{-1} and flow rate of 5 ml min^{-1}.

The WS's column sorption capacity for nitrate can be negligible, and the q_{ed} are about 0.570, 0.532 and 0.542 mg g^{-1} for bed heights of 1.0, 1.5 and 2.5 cm, respectively. Results shown in Fig. 5a indicate that the nitrate sorption capacity of AC-WS has been greatly enhanced in contrast of that of WS. The volumes of influent solution obtained for the three different bed heights at breakthrough point show that the rate of movement of the sorption zone is rapid for the smallest bed height. The movement of the sorption zone becomes reduced when the bed height is increased. As the nitrate solution continues to flow into the column, the exhaustion point on the S-shaped curve gradually approaches its exhaustion value, and it is observed that the bed volumes at the breakthrough and exhaustion points both increase as bed height increases. When the effluent nitrate concentration reaches the influent concentration, the calculated q_{ed} of AC-WS for different bed heights (1.0, 1.5 and 2.5 cm) are 87.27, 86.34 and 87.16 mg g^{-1}, respectively. Although an increased bed height corresponds to the increase in bed volume,

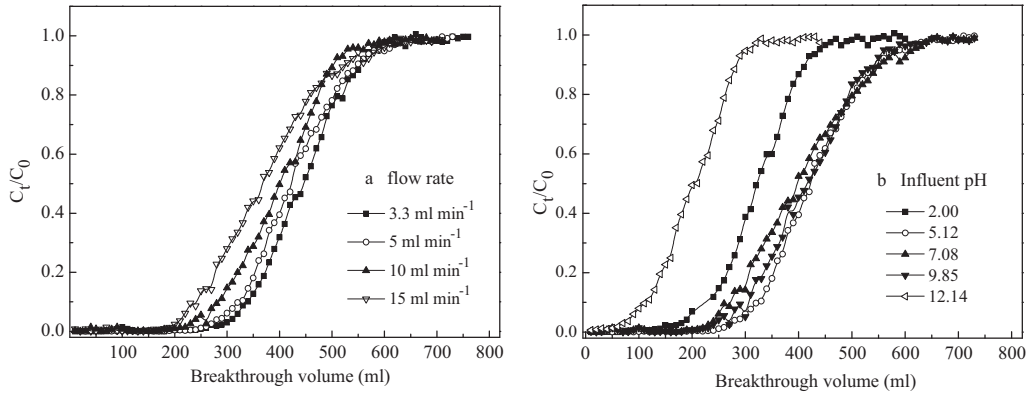

Fig. 6. Effect of flow rate and influent pH on the breakthrough curves. (a) Influent concentration: 200 mg l^{-1}, influent pH: 5.12, bed height: 1.0 cm; (b) influent concentration: 200 mg l^{-1}, bed height: 1.0 cm, flow rate: 5 ml min^{-1}.

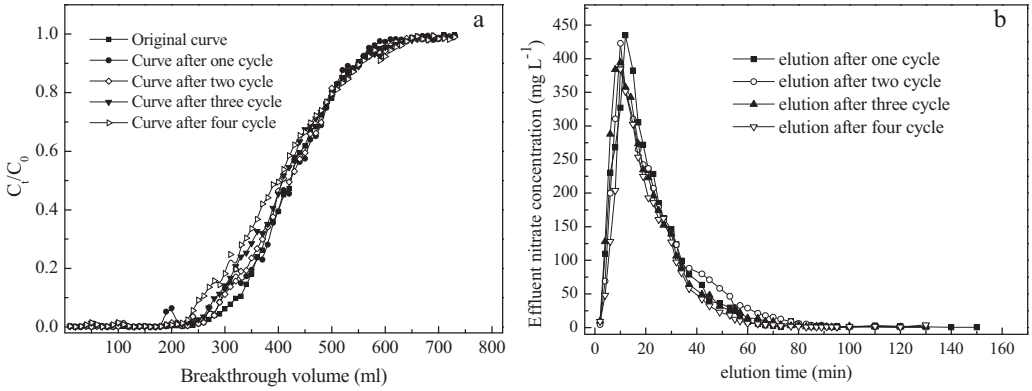

Fig. 7. Desorption and dynamic elution curves in each sorption–desorption cycle. (a) Desorption curves of AC-WS in each cycle; (b) dynamic elution curves in each curve; influent concentration: 200 mg l^{-1}, bed height: 1.0 cm, flow rate: 5 ml min^{-1}.

it is observed that effect of bed height on the q_{ed} of AC-WS can be negligible as the bed height increases from 1.0 cm to 2.5 cm.

Based on the discussion above, 1.0 cm of bed height (1.0 g of AC-WS) is selected in the following column tests.

3.2.2. Effect of influent nitrate concentration on the breakthrough curves

The breakthrough curve C_t/C_0 versus breakthrough volume treated with various initial nitrate concentrations is shown in Fig. 5b. The larger initial influent concentration, the steeper is the slope of breakthrough curve and smaller is the breakthrough volume. These results demonstrate that the change of influent concentration affects the saturation rate and breakthrough time, or in other words the diffusion process is concentration dependent [31]. As the influent concentration increases, nitrate loading rate increases which results in decrease of driving force for mass transfer for a fixed sorption zone length.

The q_{ed} of AC-WS for different initial influent concentrations (80, 120, 200 and 300 mg l^{-1}) are about 86.6, 84.3, 87.27 and 87.47 mg g^{-1}, respectively; this indicates that the influent concentration has little effect on the q_{ed} of AC-WS. Although breakthrough time is significantly decreased with the increase in influent nitrate concentration, the q_{ed} of AC-WS at higher initial concentration is still enhanced by concentration gradient with more nitrate ions adsorbed. Similar result was reported in the work of Goel [32] for the adsorption of lead (II) by treated granular activated carbon.

3.2.3. Effect of flow rate on the breakthrough curves

The experiments were conducted at bed height of 1.0 cm, at constant influent concentration of 200 mg l^{-1}, with flow rate ranging from 3.3 to 15 ml min^{-1}. Results of experiments on effect of flow rate are shown in Fig. 6a, which shows that breakthrough volume decreases from 345 to 227 ml, as flow rate increases from 3.3 to 15 ml min^{-1}. The results indicate that a decrease in flow rates at constant influent concentration of 200 mg l^{-1} increases the breakthrough volume or breakthrough time due to an increase in empty bed contact time (EBCT). The lower the EBCT, the less effective the diffusion process becomes, resulting in lower column sorption capacity for nitrate [30,31]. Thus, the packed AC-WS needs more time to bond the nitrate ions efficiently. In addition, increase in the flow rate causes increase in zone speed, resulting in a decrease in the time required to achieve breakthrough.

A decrease in q_{ed} of AC-WS from 88.18 to 82.29 mg g^{-1} is observed as the flow rate increases from 3.3 to 15 ml min^{-1}. This corresponds to the decrease in the breakthrough volume from 345 to 227 ml. Based on the discussion on the effect of flow rate, it is suggested that lower flow rate would be favor to the nitrate sorption in the column tests.

3.2.4. Effect of influent pH on the breakthrough curves

The breakthrough curve C_t/C_0 versus breakthrough volume treated with various influent pH (2.00, 5.12, 7.08, 9.85 and 12.14) is shown in Fig. 6b. As seen in Fig. 6b, the nitrate sorption capacities of AC-WS are 62.7, 87.27, 87.45, 85.15 and 41.90 mg g^{-1} for the influent pH of 2.00, 5.12, 7.08, 9.85 and 12.14, respectively. It is apparent that the nitrate sorption capacity gradually increases as the influent pH increases from 2.00 to 9.85, and then the sorption capacity significantly decreases with the further increase in pH from 9.85 to 12.14. As shown in some literature, the sorption process of some adsorbents with positive surface charges often displayed a general trend of decrease as the solution pH value increases; this may be attributed to the less attractive or more repulsive electrostatic interaction resulting from the increased negatively charged surface sites at higher solution pH values [33,34]. What's more, when the pH increases beyond 11.0, the OH^- will increase significantly, and the exchange sites for nitrate sorption will decrease on the outer surface of AC-WS due to the presence of excess OH^- ions competing with nitrate ions for sorption sites and a result of the sorption capacity decreases [35].

Based on the discussion above, it seems that the suitable influent pH range could be selected in the range of 5.0–10.0; this demonstrates a potential application for the eutrophic wastewater treatment in China, of which the pH range is about 6–9.

3.3. Desorption and dynamic elution tests

3.3.1. Desorption tests

Recovery of the adsorbed anions and repeated usability of the adsorbent is important in reference to the practical applications of treatment of industrial effluent. In this work, 0.1 mol l^{-1} of HCl solution was used as the desorption agent and its regeneration capacity after four times of sorption–desorption cycles is presented in Fig. 7a.

The q_{ed} of AC-WS at initial and after each cycle are 87.27, 86.5, 85.3, 85.4 and 83.8 mg g^{-1}, respectively. The total decrease in sorption efficiency of AC-WS after four sorption–desorption cycles is only about 5.2%, which shows that AC-WS has good potential to adsorb the nitrate from aqueous solution even when used repeatedly. In addition, HCl solution with concentration of 0.1 mol l^{-1} demonstrates the excellent desorption capacity, and the desorption of nitrate ions from the surface of AC-WS is most probably through an reaction of ion-exchange, i.e., the reverse of the reactions with high concentration of Cl^{-1} from the HCl displacing nitrate ions from AC-WS. Similar results have been reported in our previous work [18] for desorption of nitrate from agricultural by-product based anion exchanger.

3.3.2. Dynamic elution tests

In the dynamic elution tests, an elution step was carried out after each sorption–desorption cycle and the nitrate concentrations in the effluent elution solutions were determined and presented in Fig. 7b.

The elution curves from cycle 1–4 show a very similar unsymmetrical shape, with a rapid nitrate concentration increase, followed by a flatter diminution. As shown in Fig. 7b, HCl solution demonstrates a high desorption rate when eluting the nitrate ions from AC-WS. It is observed that the maximum nitrate concentration peak is achieved in about 10–15 min for all the cycles. When the elution reaches to 60 min, the effluent concentration is lower than 40 mg l^{-1}. As the desorption time reaches to 120 min, the residue nitrate concentration approaches to zero and the elution process in this cycle is finished.

Osifo et al. [36] reported a weight loss (25%) of chitosan beads after 5 sorption–desorption cycles using 0.1 mol l^{-1} of HCl solution as the desorption agent. Although a longer desorption time will be favorable to the regeneration of AC-WS, the acid elution may also increase the possibility of the destruction of cellulose/hemicellulose in AC-WS as desorption time increases; this indicates that a suitable desorption time should appropriately balance this procedure [37].

4. Conclusion

WS was modified into amine-crosslinked adsorbent after the amination reaction. Solid-state ^{13}C NMR and zeta potential analysis validated the existence of crosslinked amine groups in AC-WS. Raman shift of the nitrate peaks suggested the electrostatic attraction between the adsorbed ions and positively charged amine sites. Column sorption characteristics of AC-WS were studied and the results illustrated a potential application for the eutrophic wastewater treatment. Lower flow rate would be favor to the nitrate sorption in the column tests and the suitable influent pH range could be selected in the range of 5.0–10.0. The highest q_{ed} of AC-WS for nitrate sorption was about 87.27 mg g^{-1}. HCl solution (0.1 mol l^{-1}) demonstrated its high desorption rate for the regeneration of AC-WS. In addition, the sorption–desorption process indicated the excellent regeneration capacity of AC-WS with little loss (5.2%) in its initial sorption capacity when repeatedly used.

Acknowledgments

The research was supported by the National Natural Science Foundation of China (50878121), Key Projects in the National Science & Technology Pillar Program in the Eleventh Five-year Plan Period (2006BAJ08B05-2) and National Major Special Technological Programmes Concerning Water Pollution Control and Management in the Eleventh Five-year Plan Period (2008ZX07010-008-002).

References

[1] A. Afkhami, Adsorption and electrosorption of nitrate and nitrite on high-area carbon cloth: an approach to purification of water and waste-water samples, Carbon 41 (2003) 1309–1328.
[2] J.A. Camargo, Á. Alonso, Ecological and toxicological effects of inorganic nitrogen pollution in aquatic ecosystems: a global assessment, Environ. Int. 32 (2006) 831–849.
[3] J.A.T. Pennington, Dietary exposure models for nitrates and nitrites, Food Control 9 (1998) 385–395.
[4] B. Ovez, S. Ozgen, M. Yuksel, Biological denitrification in drinking water using *Glycyrrhiza glabra* and *Arunda donax* as the carbon source, Process Biochem. 41 (2006) 1539–1544.
[5] B. Ovez, Batch biological denitrification using *Arundo donax*, *Glycyrrhiza glabra*, and *Gracilaria verrucosa* as carbon source, Process Biochem. 41 (2006) 1289–1295.
[6] Y.H Huang, T.C. Zhang, Nitrite reduction and formation of corrosion coatings in zerovalent iron systems, Chemosphere 64 (2006) 937–943.
[7] M.A. Ben Ali, M. Rakib, S. Laborie, P. Viers, G. Durand, Coupling of bipolar membrane electrodialysis and ammonia stripping for direct treatment of wastewaters containing ammonium nitrate, J. Membr. Sci. 244 (2004) 89–96.
[8] C.D. Rocca, V. Belgiorno, S. Meriç, Overview of *in-situ* applicable nitrate removal processes, Desalination 204 (2007) 46–62.
[9] M. Chabani, A. Amrane, A. Bensmaili, Kinetics of nitrate adsorption on Amberlite IRA 400 resin, Desalination 206 (2007) 560–567.
[10] R. Saad, K. Belkacemi, S. Hamoudi, Adsorption of phosphate and nitrate anions on ammonium-functionalized MCM-48: effects of experimental conditions, J. Colloid Inter. Sci. 311 (2007) 375–381.
[11] P. Nigam, G. Armour, I.M. Banat, D. Singh, Physical removal of tectile dyes from effluents and solid-state fermentation of dye-adsorbed agricultural residues, Bioresour. Technol. 72 (2000) 219–226.
[12] U.S. Orlando, A.U. Baes, W. Nishijima, Preparation of agricultural residue anion exchangers and its nitrate maximum adsorption capacity, Chemosphere 48 (2002) 1041–1046.
[13] U.S. Orlando, A.U. Baes, W. Nishijima, M. Okada, A new procedure to produce lignocellulosic anion exchangers from agricultural waste materials, Bioresour. Technol. 83 (2002) 195–198.
[14] U.S. Orlando, A.U. Baes, W. Nishijima, M. Okada, Comparative effectivity of different types of neutral chelating agents for preparing chelated bagasse in solvent-free conditions, J. Clean. Prod. 12 (2004) 753–757.
[15] U.S. Orlando, T. Okuda, W. Nishijima, Chemical properties of anion exchangers prepared from waste natural materials, React. Funct. Polym. 55 (2003) 311–318.
[16] A. Biswas, B.C. Saha, J.W. Lawton, R.L. Shogren, J.L. Willett, Process for obtaining cellulose acetate from agricultural by-products, Carbohydr. Polym. 64 (2006) 134–137.
[17] M.M. Ibrahim, A. Dufresne, W.K. El-Zawawy, F.A. Agblevor, Banana fibers and microfibrils as lignocellulosic reinforcements in polymer composites, Carbohydr. Polym. 81 (2010) 811–819.
[18] X. Xu, B.Y. Gao, Q.Y. Yue, Q.Q. Zhong, Preparation of agricultural by-product based anion exchanger and its utilization for nitrate and phosphate removal, Bioresour. Technol. 101 (2010) 8558–8564.
[19] R.R. Navarro, S. Katsushiro, F. Naoyuki, M. Matsumura, Mercury removal from wastewater using porous cellulose carrier modified with polyethyleneimine, Water Res. 30 (1996) 2488–2494.
[20] N. Biçak, B.F. Şenkal, Removal of nitrite ions from aqueous solutions by cross-linked polymer of ethylediamine with epichlorohydrin, React. Funct. Polym. 36 (1998) 71–77.
[21] X. Xu, B.Y. Gao, Q.Y. Yue, Q.Q. Zhong, Preparation and utilization of wheat straw bearing amine groups for the sorption of acid and reactive dyes from aqueous solutions, J. Hazard. Mater. 182 (2010) 1–9.
[22] R.H. Newman, R.J. Redgwell, Cell wall changes in ripening kiwifruit: ^{13}C solid state NMR characterisation of relatively rigid cell wall polymers, Carbohydr. Polym. 49 (2002) 121–129.
[23] V. Singh, A.K. Sharma, D.N. Tripathi, R. Sanghi, Poly(methylmethacrylate) grafted chitosan: an efficient adsorbent for anionic azo dyes, J. Hazard. Mater. 161 (2009) 955–966.
[24] A. Baraka, P.J. Hall, M.J. Heslop, Preparation and characterization of melamine formaldehyde–DTPA chelating resin and its use as an adsorbent for heavy metals removal from wastewater, React. Funct. Polym. 67 (2007) 585–600.
[25] M.A. Martins, L.A. Forato, L.H.C. Mattoso, L.A. Colnago, A solid state ^{13}C high resolution NMR study of raw and chemically treated sisal fibers, Carbohydr. Polym. 64 (2006) 127–133.
[26] I.H. Yoon, X.G. Meng, C. Wang, K.W. Kim, S. Bang, E. Choe, L. Lippincott, Perchlorate adsorption and desorption on activated carbon and anion exchange resin, J. Hazard. Mater. 164 (2009) 87–94.
[27] S.W. Ellepola, S.-M. Choi, D.L. Phillips, C.-Y. Ma, Raman spectroscopic study of rice globulin, J. Cereal Sci. 43 (2006) 85–93.
[28] A.M. Oliveira, V.A. Leão, C.A. da Silva, A proposed mechanism for nitrate and thiocyanate elution of strong-base ion exchange resins loaded with copper and gold cyanocomplexes, React. Funct. Polym. 68 (2008) 141–152.
[29] J. Hu, G.H. Chen, I.M.C. Lo, Removal and recovery of Cr(VI) from wastewater by maghemite nanoparticles, Water Res. 39 (2005) 4528–4536.
[30] P. Suksabye, P. Thiravetyan, W. Nakbanpote, Column study of chromium(VI) adsorption from electroplating industry by coconut coir pith, J. Hazard. Mater. 160 (2008) 56–62.
[31] M.K. Mondal, Removal of Pb (II) ions from aqueous solution using activated tea waste: adsorption on a fixed-bed column, J. Environ. Manage. 90 (2009) 3266–3271.
[32] J. Goel, K. Kadirvelu, C. Rajagopal, V.K. Garg, Removal of lead (II) by adsorption using treated granular activated carbon: batch and column studies, J. Hazard. Mater. 125 (2005) 211–220.
[33] A. Ozcan, A.S. Ozcan, Adsorption of acid red 57 from aqueous solutions onto surfactant-modified sepiolite, J. Hazard. Mater. 125 (2005) 252–259.
[34] P.K. Malik, Use of activated carbons prepared from sawdust and rice-husk for adsorption of acid dyes: a case study of Acid Yellow 36, Dyes Pigments 56 (2003) 239–249.
[35] R. Chand, T. Watari, K. Inoue, T. Torikai, M. Yada, Evaluation of wheat straw and barley straw carbon for Cr (VI) adsorption, Sep. Purif. Technol. 65 (2009) 331–336.
[36] P.O. Osifo, H.W.J.P. Neomagus, R.C. Everson, A. Webster, M.A. vd Gun, The adsorption of copper in a packed-bed of chitosan beads: modeling, multiple adsorption and regeneration, J. Hazard. Mater. 167 (2009) 1242–1245.
[37] N. Kuyucak, B. Volesky, Desorption of cobalt-laden algal biosorbent, Biotechnol. Bioeng. 33 (1989) 815–822.